COBEM 2021 26th International Congress of Mechanical Engineering
November 22-26, 2021, Virtual Congress, Brazil

COB-2021-1355
A MODIFIED WINDKESSEL MODEL APPLIED IN A TUBULAR PULSATION DAMPENER ANALYSIS

Michel de Oliveira dos Santos
Instituto Federal do Espírito Santo – *Campus* São Mateus – Rodovia BR 101 Norte, km 58 – Litorâneo – CEP 29.932-540 – São Mateus – ES
michel.saints@gmail.com

Daniel da Cunha Ribeiro
Universidade Federal do Espírito Santo – *Campus* São Mateus – Rodovia BR 101 Norte, km 60 – Litorâneo – CEP 29.932-540 – São Mateus – ES
gottfried.leibnitz@gmail.com

João Paulo Barbosa
Instituto Federal do Espírito Santo – *Campus* São Mateus – Rodovia BR 101 Norte, km 58 – Litorâneo – CEP 29.932-540 – São Mateus – ES
joaopauloengmec@gmail.com

Renato do Nascimento Siqueira
Instituto Federal do Espírito Santo – *Campus* São Mateus – Rodovia BR 101 Norte, km 58 – Litorâneo – CEP 29.932-540 – São Mateus – ES
renatons.ifes@gmail.com

Abstract. *In this work, the two-parameter Windkessel model, a model widely used in the area of hemodynamics, was used to determine the behavior of a tubular pulsation dampener, with deformable latex walls, installed in a hydraulic circuit powered by a positive displacement pump. Pulsation dampeners or accumulators are devices widely used in industrial pumping systems to reduce pressure and flow pulsations that generate excessive noise, undesirable mechanical vibrations and process instabilities. In conventional pulsation dampeners, compressed gases are used as a continuous deformable medium, with pure nitrogen and dry air being the most common gases. However, to achieve greater reliability, an accumulator can be designed to dispense the compressed gas, as long as it provides the same level of pressure and flow attenuation in a suitable frequency range. At first, the Windkessel model was modified to consider the variable flow resistance due to the turbulent regime, but keeping constant dampener compliance. In sequence, another modification was made to consider the pressure-dependent pulsation dampener compliance. To estimate compliance as a pressure function, by means of simulations using the finite element method a relationship between accumulator volume variation and an average internal pressure related to steady state flow Reynolds number was determined. The results of two modified models were compared in terms of attenuation (ratio between flow amplitude before and after the pulsation dampener) and dampener volume change. Non-linear ordinary differential equations resulting from modified models were solved for time averaged Reynolds number range from 16000 to 24000 and Strouhal number from 0.01 to 0.13. Results demonstrated that an increase in both Reynolds and Strouhal number resulted in greater attenuation of flow amplitude. Also greater attenuation was achieved in variable compliance model (maximum value of 4.72) than constant compliance model (maximum value of 3.07). Regarding dampener volume change, it was verified that it mainly decreases for a Strouhal number increase. In general, best theoretical behavior of the dampener (higher attenuations and lower volume changes) was found for higher values of both Reynolds and Strouhal number for evaluated ranges.*

Keywords: *Pulsation dampeners, Windkessel model, intermittent flow, hydraulic systems modeling, finite element method.*

1. INTRODUCTION

Pulsation dampeners (or accumulators) are devices widely used to reduce pressure pulsations that occur in industrial pumping systems (Xiaohui et al., 2015; Koegler *et al*., 2017, Shi *et al*., 2019, Xu *et al*., 2019). They can also be used in systems whose instabilities are caused by two-phase flows, such as in steam generators and condensers (Liang *et al*., 2020). Naturally, by decreasing the pressure fluctuation amplitudes, the attenuator contributes to time stabilization flow rate, which also has intermittent characteristics. By reducing the pulsed flow, the attenuator protects

the piping system from mechanical fatigue, also protecting and facilitating the operation of measuring instruments installed in the line, among other advantages. The use of attenuators is very common in hydraulic systems that have the driving force coming from positive displacement pumps, especially those who rely on alternative principle, such as piston and diaphragm (Xu *et al*., 2018; Zuti *et al.*, 2019).

Dampener working principle is based on the transference mechanism of the mechanical energy initially present in transported fluid to a continuous medium (a fluid or a solid) that has a considerable energy storage capacity due to its deformation. Thus, the mechanical energy that instantly exceeds the average levels, and that is associated with pressure peaks in an intermittent flow, can be temporarily stored in the continuous deformable medium and later almost entirely (there are always irreversibilities in this process) returned to transported fluid when the pressure plateau in the flow is reduced. This cycle of removal, storage and return of mechanical energy promotes time stabilization and reduction of pressure and flow fluctuations in intermittent flows. In analogy to dynamic mechanical systems, such as the vehicle suspension, the continuous deformable medium plays the role of a spring, which deforms when the wheel passes over a disturbance in the path, whether a bump or a hole, resulting in a restoring force that returns the wheel to equilibrium position when the disturbance ceases (Rao, 2009). In analogy to electrical systems, the attenuator has a similar function of a capacitor, and this analogy, when extended to other elements of a hydraulic system, is a very common way of modeling physical behavior (Wachel and Price, 1988; Westerhof *et al*., 2008).

In conventional dampeners, compressed gases are used as a continuous deformable medium. The most commonly used gases are pure nitrogen (N_2) and dry air. The gas is separated from the fluid by a relatively thin membrane, usually made of highly deformable elastomeric material such nitrile rubber. In these dampeners, given the operating conditions, fundamentals of thermodynamics related to gas compression processes are used to determine basic project parameters, such as total volume and pressure variation in the gas (Wu *et al*., 2019).

There are several dampener types, with their particular advantages and disadvantages, which are presented and discussed in the classic work of Wachel and Price (1988) based on simulations of their applications in a typical hydraulic system. However, almost all dampeners shares the fact that performance is very sensitive to the initial pressure of the gas, since this pressure, along with the dampener volume, defines the ability to reduce fluctuations of pressure and flow rate through the storage and return mechanism described above.

Once the attenuator is installed in hydraulic system, disregarding other adverse events such as the eventual rupture of elastic membrane, the attenuator efficiency becomes dependent on the maintenance of the gas pressure at values close to those prescribed in project phase. In most known systems, such maintenance can be done without major hindrances. However, in some engineering areas like offshore oil exploration, there is always a demand for the technological evolution of devices in order to achieve an extreme high degree of reliability and very low need of maintenance, since any interventions in equipment under large water depths are difficult to carry out and very costly above all. Another important fact for offshore installations is limited space that demands compact designs of equipments. From this perspective, the concept of a dampener that operates without the need for a volume of gas is interesting, as long as this device still owns the ability to attenuate the pressure/flow in appropriate operating frequency range, and is compact enough to fit most systems without major changes.

Elements that operate as dampeners, storing mechanical energy of pulsed flow in a deformable membrane, are very common in the area of hemodynamics, a branch of medicine that intersects with engineering and basically studies fluid dynamics in circulatory system and its implications (Ku, 1997; Thomas and Sumam, 2015). A classic example is the aorta artery, which is located immediately after the heart. Due to the fact that the aorta artery has a considerably larger diameter than other arteries, it contributes to a reduction in peak pressure in the rest of the circulatory system during systole and even during diastole, where the heart does not drive the blood, flow is maintained in the most of other arteries. The ability to store and return mechanical energy through volume variation is called compliance.

Literature demonstrates that many analysis and models used in hemodynamics area can be extended to operating conditions of industrial hydraulic systems and contribute to development of design methodology and optimization of the new attenuator proposal. Concentrated parameter models, such as the Windkessel model (Westerhof *et al*., 2008; Gostuski *et al*., 2016) and its variations (Aboelkassem and Virag, 2019) can be used for initial studies of dampener behavior. During a later stage of device development, more complex models that use advanced computational tools such as computational fluid dynamics (CFD) and finite element method for structural analysis (FEM) techniques can be used to refine the value ranges for the possible variables involved and optimize the device behavior (Lorenzini and Conti, 2013; Alimohammadi *et al*., 2015; Jahangiri *et al*., 2017; Nowak *et al*., 2019).

In this work, two-element (flow resistance R and dampener compliance C) Windkessel model was used to predict the behavior of a tubular dampener with a flexible latex wall, installed in a hydraulic circuit subjected to an intermittent flow rate with periodic characteristic. The dampener compliance estimation was made using two models: 1) constant compliance model as presented by Mei *et al*. (2018); and 2) variable compliance model by means of simulations using the finite element method, were was determined a relationship between accumulator volume variation and an average internal pressure related to steady state flow Reynolds number. The ability to reduce the flow amplitude as a function of a time averaged Reynolds number ($\overline{Re}$) and Strouhal number (St) was evaluated. Dampener volume change was also estimated. Since the Windkessel model is a linear model (initially developed to analyze laminar flows and constant

attenuator compliance condition), two modifications to the model were proposed to analyze a turbulent flow range and a condition where the hydraulic dampener has variable compliance.

2. METHODOLOGY

The two-element Windkessel model, expressed by Eq. (1), seeks to represent the behavior of a fluid dynamic system with intermittent flow by means of a mass balance and defining the input and output flows of the dampener element in terms of two main properties of the simplified system: the flow resistance *R*, a characteristic of hydraulic system, and the compliance *C*, main dampener characteristic:

$$Q_P(t) = Q_D(t) + Q_R(t) = C\frac{dp(t)}{dt} + \frac{p(t)}{R}, \tag{1}$$

where *t* is time, $Q_P(t)$ is the flow rate at pump exit, $Q_D(t)$ is the flow rate instantaneously stored or liberated by dampener due to volume variation, $Q_R(t)$ is the flow rate that goes through hydraulic system and is submitted to pressure and flow attenuation, $p(t)=p$ is the pump exit pressure, also considered as dampener inside pressure, because is highly recommended that dampener installation be made as near as possible from pump exit, so pressure drop between this two devices can be neglected. Figure 1 is a representation of electric circuit analogy for two-element Windkessel model, where *P* represents the pump and p_{atm} is the atmospheric pressure at hydraulic system exit.

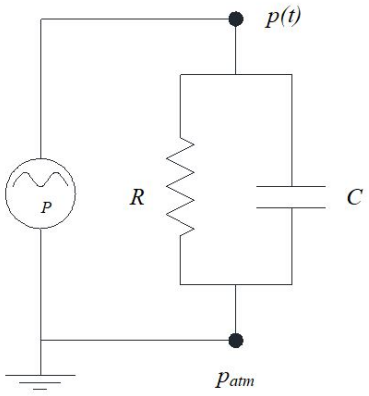

Figure 1. Schematic representation of electric circuit analogy for two-element Windkessel model.

When *R* and *C* are constants (laminar flow and linear behavior of dampener), the model has an analytical solution. Mei *et al*. (2018) demonstrated that Windkessel model is in fact a simplified approach of more generalized problem of flow through a deformable tube, but this analysis was still made for laminar flow. To consider the variation of *R* when the flow occurs in turbulent conditions, the model was rewritten in terms of time variable Reynolds number *Re*, according to the development presented in Eq. (2) to Eq. (12). Despite the possibility of using harmonic series to compose a more generalized form of $Q_P(t)$ for model input, as done by Mei *et al*. (2018), in this work, a simple harmonic form was considered, composed of the time averaged flow rate $\bar{Q}$ and its amplitude Q':

$$U(t) = U = \frac{\nu}{D}Re(t) = \frac{\nu}{D}Re, \tag{2}$$

$$Re(t) = Re = \frac{4}{\pi\nu D}Q, \tag{3}$$

$$\overline{Re} = \frac{4\bar{Q}}{\nu\pi D}, \tag{4}$$

$$r_Q = \frac{Q'}{\bar{Q}}, \tag{5}$$

$$Q_P(t) = \bar{Q} + Q'cos(\omega t) = \bar{Q}\left(1 + r_Q cos(\omega t)\right) = \frac{\nu\pi D}{4}\overline{Re}\left(1 + r_Q cos(\omega t)\right), \tag{6}$$

$$p(t) = p = f(Re)\rho\frac{L_e}{2D}U^2 = aRe^b\rho\nu^2\frac{L_e}{2D^3}Re^2 = a\rho\nu^2\frac{L_e}{2D^3}Re^{2+b}, \tag{7}$$

$$Q_D(t) = C\frac{dp}{dt} = C\left(\frac{dp}{dRe}\frac{dRe}{dt}\right) = C[a(2+b)]\rho\nu^2\frac{L_e}{2D^3}Re^{1+b}\frac{dRe}{dt}, \tag{8}$$

$$R = \frac{dp}{dQ} = \frac{dp}{dRe}\frac{dRe}{dQ} = a(2+b)\rho\nu^2\frac{L_e}{2D^3}Re^{1+b}\frac{4}{\pi\nu D}, \tag{9}$$

$$Q_R(t) = \frac{p}{R} = \left(a\rho\nu^2 \frac{L_e}{2D^3} Re^{2+b}\right) / \left(a(2+b)\rho\nu^2 \frac{L_e}{2D^3} Re^{1+b} \frac{4}{\pi\nu D}\right) = \frac{\pi\nu D}{(4+2b)} Re, \tag{10}$$

$$St = \frac{\omega D}{\bar{U}}, \tag{11}$$

$$\omega = St\overline{Re}\frac{\nu}{D^2}, \tag{12}$$

where $\overline{Re}$ is the time averaged Reynolds number, U is the instantaneous area average velocity, ν is the fluid cinematic viscosity, ρ is fluid density, D is the tube diameter, r_Q is the ratio of flow rate amplitude, ω is the angular frequency, f is de friction factor as function of Re, a and b are the coefficients of Blasius type correlation for f, L_e is the equivalent length of hydraulic system (same as used for total pressure drop determination, with contribution of distributed and localized pressure drop elements). With presented definitions from Eq. (2) to Eq. (12), Eq. (1) was rewritten as Eq. (13), a non linear model that was numeric solved for time dependent Re, using information about hydraulic system, dampener compliance, fluid proprieties and primary flow conditions (average flow rate and frequency).

$$\frac{\nu\pi D}{4}\overline{Re}\left(1 + r_Q cos\left(St\overline{Re}\frac{\nu}{D^2}t\right)\right) = C[a(2+b)]\rho\nu^2 \frac{L_e}{2D^3} Re^{1+b} \frac{dRe}{dt} + \frac{\pi\nu D}{(4+2b)} Re. \tag{13}$$

The pulsation dampener compliance C was determined based on physical properties and dimensions of an elastic tube, using a model proposed by Mei *et al*. (2018), given by Eq. (14). Table 1 presents the values used for C determination and the parameters values used in the modified Windkessel model given by Eq. (13). All these values are related to an experiment of a prototype tubular pulsation dampener made of latex installed in hydraulic system powered by a positive displacement pump that is current running by the authors.

$$C = \frac{\pi r_D^3 L_D}{E h_D}, \tag{14}$$

where E is the dampener wall material Young's modulus, r_D, L_D and h_D are the dampener radius, length and wall thickness respectively.

Table 1. Values used in the Windkessel modified model.

Parameter	Value
E, MPa	4.13
r_D, mm	20.00
L_D, mm	300.00
h_D, mm	0.50
C, mm^3/Pa	7.31
ν, m^2/s	8.93×10^{-7}
ρ, kg/m^3	997
D, mm	20.93
L_e, m	25.64
a	0.302
b	-0.248

In addition to the result obtained by Eq. (14), dampener compliance estimative was made based on a numerical experiment using the finite element method (FEM), in which dampener was subjected to internal pressure and volume variation was determined. Applied pressure values was estimated based on permanent flow characterized by $\overline{Re}$ value in the considered hydraulic system. A range of $\overline{Re}$ from 4000 to 24000 was evaluated. A mesh of linear tetrahedral elements with 9604 nodes was used for geometry discretization. The material was considered to have linear elastic behavior, with E value given in Table 1. Applied boundary conditions were zero displacement across the entire contour of the tube at both ends. The simulations were implemented in the Ansys® Workbench 2021 R1 software. From the displacement of the wall, the increase of dampener volume ΔV_D was determined. The increase of volume was related to the value of $\overline{Re}$ by means of quadratic model, given by Eq. (15), with a high determination coefficient value of 0.998. Furthermore, an analysis of variance performed on the model residuals showed that all assumed coefficients are significant at the 5% level. Figure 2 presents the results of ΔV_D and the fitted model curve. The coefficient values of A, B and F are 1.14266×10^{-5} m^3, -2.33605×10^{-9} m^3 and 3.45062×10^{-9} m^3, respectively. The compliance as a function of $\overline{Re}$, obtained from the numerical experiment $C_{\overline{Re}}$, was determined from the derivative of Eq. (15) in relation to $\overline{Re}$, according to Eq. (16):

$$\Delta V_D = A + B\overline{Re} + F\overline{Re}^2, \tag{15}$$

$$C_{\overline{Re}} = \frac{d(\Delta V_D)}{d\overline{Re}} = B + 2F\overline{Re}. \tag{16}$$

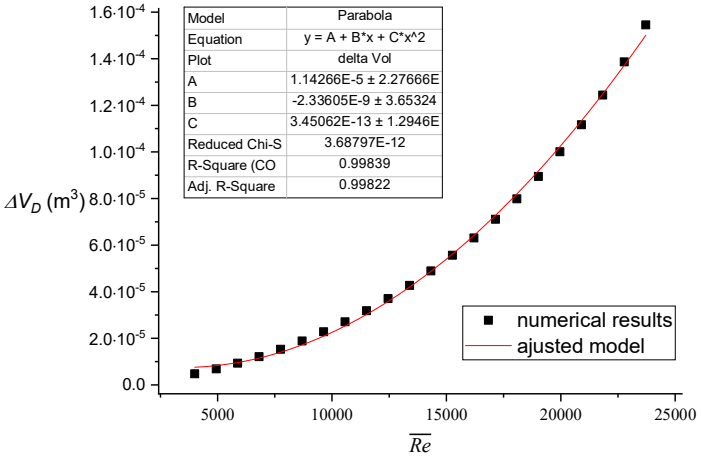

Figure 2. Numerical results of ΔV_D and adjusted model for $\Delta V_D(\overline{Re})$.

By definition, C represents instantaneous dampener volume variation in relation to pressure. Thus, for application of Eq. (16) in previous modified Windkessel model, another change was made in the term $Q_C(t)$, as described in Eq. (17). The adapted model is presented in Eq. (18):

$$C\frac{dp}{dt} = \frac{d(\Delta V_D)}{dp}\frac{dp}{dt} = \frac{d(\Delta V_D)}{dp}\left(\frac{dp}{dRe}\frac{dRe}{dt}\right) = \frac{d(\Delta V_D)}{dRe}\frac{dRe}{dt} = C_{Re}\frac{dRe}{dt} = (B + 2FRe)\frac{dRe}{dt}, \tag{17}$$

$$\frac{\nu\pi D}{4}\overline{Re}\left(1 + r_Q cos\left(St\overline{Re}\frac{\nu}{D^2}t\right)\right) = (B + 2FRe)\frac{dRe}{dt} + \frac{\pi\nu D}{(4+2b)}Re. \tag{18}$$

For the last step given in Eq. (16), it was assumed that $C_{Re} = C_{\overline{Re}}$, and this means that a model adjusted for a property description in steady state flow characterized by $\overline{Re}$ is used in a dynamic application. This is acceptable in this case due to the dampener little mass, so there is no considerable delay between changes in Re (or pressure) and changes in dampener volume. This is the same principle applied to the most of vibrations analysis when a stiffness of a spring, a static determined parameter, is used to describe force and displacement relation even in a dynamic model (Rao, 2009).

Thus, two models were evaluated: the model given by Eq. (13) for constant C, and the model given by Eq. (18) for variable C. As both models result in nonlinear differential equations, the solutions were obtained by numerical techniques, using the Adams predictor-corrector method. The implementation of the solution code and other operations necessary to obtain the results were made with Scilab 6.1.0 software. Results were obtained for $\overline{Re}$ range from 16000 to 24000 and for St range from 0.01 to 0.13. The $\overline{Re}$ and St ranges were selected for being close to the experimental ranges being evaluated and based in the work of Ribas and Deschamps (2004), who demonstrated that, for those ranges, the dynamic effects of pressure and flow fluctuations do not critically influence the friction factor f, so that this parameter can still be related only to Re, without considerable errors. As St increases, f turns to be a function not only of Re but also dependant of flow acceleration and deceleration, so a simple relationship like Blasius correlation form can not be used. Effects of different r_Q (0.25 and 0.50) were also evaluated using both models.

The attenuator behavior was evaluated by determining two parameters: 1) the attenuation a_D, which represents the ratio between the amplitude of Q_P and the amplitude of Q_R, when stable conditions are reached, according to Eq. (19); and 2) the volume change ratio R_V, which represents the ratio between the dampener volume change and the initial volume when stable conditions are reached, according to Eq. (20):

$$a_D = \left(\int_{t_1}^{t_1+\tau}\sqrt{(Q_P - \bar{Q})^2}\right)/\left(\int_{t_1}^{t_1+\tau}\sqrt{(Q_R - \bar{Q})^2}\right), \tag{19}$$

$$R_V = \frac{\left(\int_{t_1}^{t_1+\tau}\sqrt{(Q_D)^2}\right)}{2V_0}, \tag{20}$$

where t_1 is the time determined when stable conditions are achieved and no more changes are observed in dampened flow rate amplitude, τ is a oscillation period ($\tau = 2\pi/\omega$) and V_0 is the undeformed dampener volume. The results of a_D and R_V were plotted as contours in terms of $\overline{Re}$ and St.

3. RESULTS AND DISCUSSION

Figure 3 shows the dampener behavior in relation to achieved attenuation a_D, in a comparison between two modified Windkessel models. It is observed that the attenuation was greater when the compliance C was considered variable and estimated from the numerical experiment using FEM. This result is attributed to the fact that the numerical estimate of dampener compliance for the evaluated $\overline{Re}$ range provided values of C greater than the value estimated by the Mei *et al.* (2018) model (from approximately 9.3 mm^3/Pa to 14.8 mm^3/Pa). In fact, variations in radius due to deformation in cylindrical geometries result in increasingly larger volume variations as the radius itself increases. This explains how compliance increases with Re according to the obtained model expressed by Eq. (15), even when in numerical model the deformations are not uniformly distributed due to boundary conditions. However, the effect of C variation with Re is also present and can be seen in Figure 4, which presents the ratio between the attenuations obtained in each model. If only an increase or decrease of C between the models is made, the ratio between the results would be constant. On the other hand, although C instantly reached values 1.71 times larger than the value related to constant C model, the maximum attenuation in variable C model was limited to 1.54 times the maximum attenuation obtained in the constant C model. Considering this non-linear behavior is important for dampener design, because, if compliance is variable, a change in this parameter does not change attenuation with same intensity, as expected in the purely linear model.

In Figure 3, it is also observed that in both models, the attenuation increases along with $\overline{Re}$ and St. The highest a_D value obtained for constant C ($\overline{Re}$ = 24000 and St = 0.13) was 3.069, while the highest value obtained for variable C model was 53% higher (4.719). Regarding attenuation, a comparison between different r_Q is not presented because there was no effect of changing this parameter on these results, indicating the independence of the attenuation in relation to this parameter. This fact was easily observed by making the ratio between each result of a_D for r_Q = 0.50 over the respective result for r_Q = 0.25, and obtaining values very close to 1, with small deviations that can be associated with the numerical method. Therefore, the attenuation independence of r_Q can only be stated for cases that input flow rate is composed by only one harmonic component, like assumed for Q_P. More general situations regarding other descriptions of input flow rate need to be evaluated.

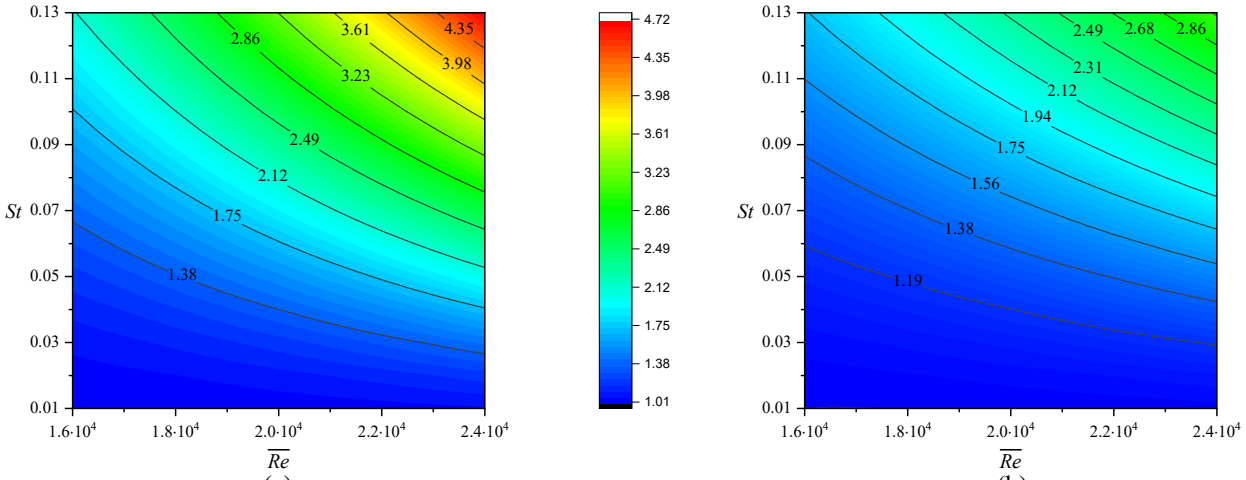

Figure 3. Attenuation a_D as function of $\overline{Re}$ and St for r_Q = 0.25: (a) variable C and (b) constant C.

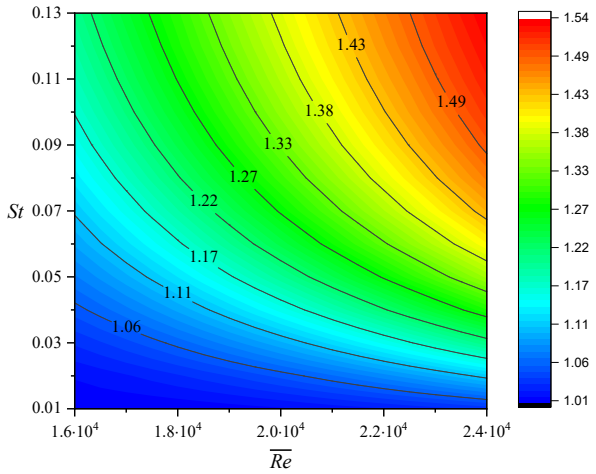

Figure 4. Distribution of ratio between results for a_D in variable C model and a_D in constant C model.

Figure 5 shows the behavior of dampener volume change ratio R_V in constant C model. Unlike a_D, R_V increases along St reduction, however, due to a $\overline{Re}$ increase, R_V also increases. Thus, maximum value for evaluated ranges (0.41) occur at $\overline{Re}$ = 24000 and St = 0.01. It is also observed that R_V becomes more sensitive to the variation of $\overline{Re}$ for smaller values of St. This can be easily observed when a constant St line is traced and noticing that this line crosses more R_V contours for a lower St value. Regarding the different r_Q values, it is observed that the increase in R_V occurs in the same proportion as the increase in r_Q. Figure 6 shows contour lines of R_V for variable C model, were the same observations can be made about the behavior related to $\overline{Re}$ and St.

Coupled analysis of a_D and R_V general behavior using the two models allows us to infer that the dampener presents more desirable behavior when operating at higher values of St, since the attenuations achieved are greater and the device presents smaller changes in volume. However, it is important to highlight that higher values of St, generally associated with higher values of ω, may result in considerable deviations between the predicted and real behavior of device. Gebreegziabher et al. (2011) reported particular behaviors of the high frequency pulsatile flow, like the one related to friction factor, which tends to show greater differences from friction factor related to quasi-static flow as the values of ω increase.

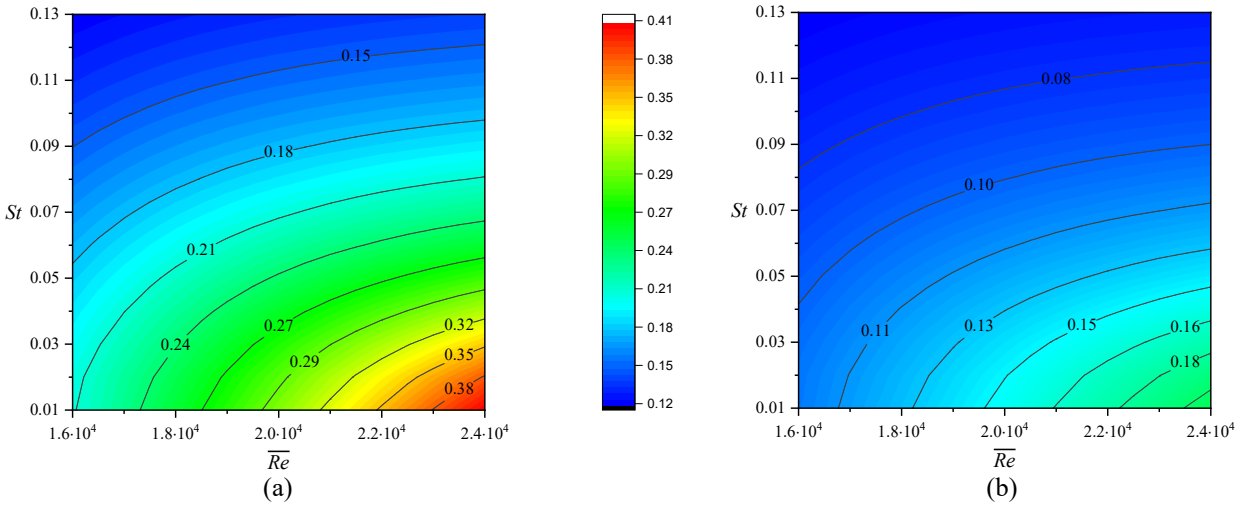

Figure 5. R_V as function of $\overline{Re}$ and St for constant C: (a) r_Q = 0.50 and (b) r_Q = 0.25.

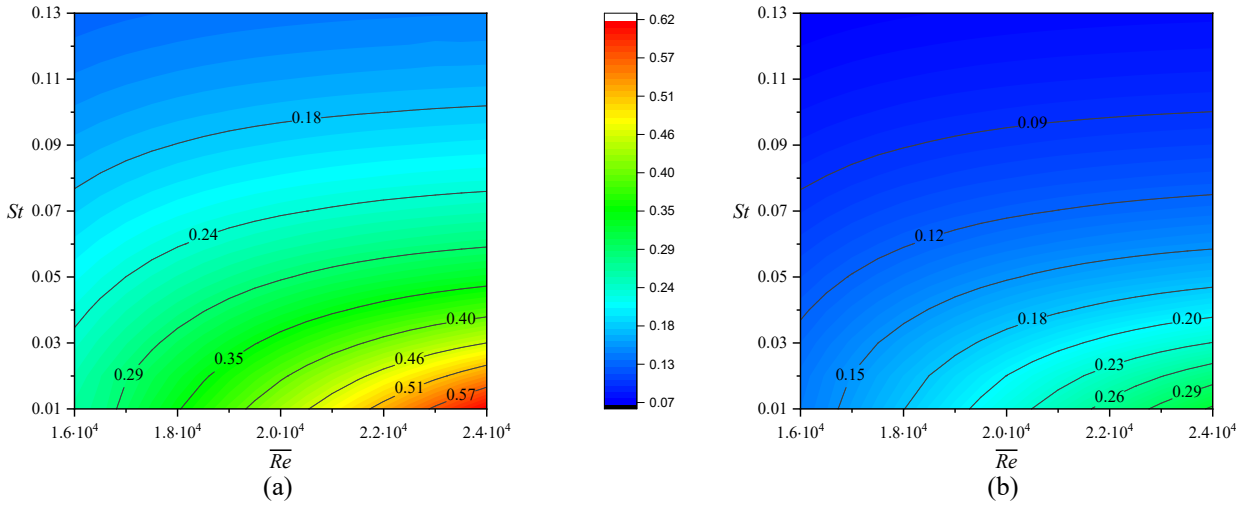

Figure 6. R_V as function of $\overline{Re}$ and St for variable C: (a) $r_Q = 0.50$ and (b) $r_Q = 0.25$.

For evaluation of compliance effect, made from comparison between Figures 5 and 6, it is observed that a higher value of C results in a higher R_V and the effect of C variation as a function of Re resulted in a lower sensitivity to $\overline{Re}$ for smaller values of St. This can be seen in the shape change that follows change in position of contours. While the change in position of contours is associated with the value of C, the change in shape of contour is associated with the variability of C with Re, which results in a change in the gradient of R_V related to $\overline{Re}$. A better perception of C variability effect on R_V can be seen from the ratio between the results presented in Figure 5(a) over the results presented in Figure 5(b), as shown in Figure 7. Results for variable C model was overall higher than results for constant C model, an this fact could be assigned to the highest estimate of C in the range of $\overline{Re}$ evaluated. However, the distribution of increased values occurs as a function not only of $\overline{Re}$, but also of St. The increase in $\overline{Re}$ and the decrease in St results in greater differences between the two models.

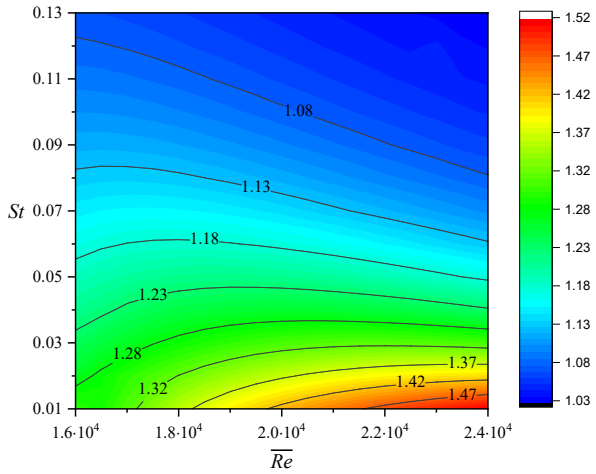

Figure 7. Distribution of ratio between results for R_V in variable C model and R_V in constant C model.

The importance of evaluating the RV parameter in the design of the damper can be highlighted in the following aspects: 1) large volume variations indicate large deformations and higher stresses to which the attenuator material will be submitted, indicating a greater possibility of mechanical failure of the component; 2) larger deformations are responsible for larger deviations from the assumed linear behavior for the material in both models (constant C and variable C), which can make the use of the models unfeasible in certain situations, reinforcing the need for comparison with experimental results to assess this behavior as well as the attenuation results. 3) even if it were assumed the occurrence of large deformations for the device and all the implications in the modeling and prediction of attenuation levels, the consideration of the volume change must be made to determine possible contact interferences between the dampener and the rigid elements of a possible safety system covering the dampener. Such interferences radically changes the dampener compliance behavior and the system response, being, therefore, a relevant point to be analyzed in future works, along with others such as the behavior of non-linear materials.

4. CONCLUDING REMARKS

This work used two-element Windkessel model, with two modifications, to theoretically analyze the behavior of tubular hydraulic dampener, with emphasis on flow rate attenuation. The first modification described was made to allow an analysis in turbulent flow range and considering constant *C*, while the second modification allowed the use of variable C model, obtained by means of numerical simulations with FEM.

In both models (constant *C* and variable *C*), a_D attenuation increased with $\overline{Re}$ and *St*, with higher values obtained for the variable *C* model, since in this model the values of instantaneous *C* varied in a higher range (between 5.4 mm^3/Pa and 12.1 mm^3/Pa when determined using *Re*) than the value related to constant *C* model (7.31 mm^3/Pa). However, the verified attenuation increase was not proportional to the increase in *C*, evidencing a non-linear characteristic of the model that considers the variation of this parameter.

In both models, the dampener was subjected to increasing volume changes along with $\overline{Re}$ increase and *St* decrease. Considering the attenuation and volume change behaviors, for evaluated ranges of $\overline{Re}$ and *St*, the tubular hydraulic dampener performed better at higher values of *St*, which resulted in greater attenuation at the cost of less volume change. The importance that all results presented could be compared with experimental data is highlighted, and future works can explore other conditions of operation of the attenuator, such as $\overline{Re}$ and *St* greater ranges, limitations imposed on volume variation and non-linear behaviors of material modulus of elasticity that may impact compliance.

5. REFERENCES

Aboelkassem, Y., Virag, Z., 2019. "A hybrid Windkessel-Womersley model for blood flow in arteries". *Journal of Theoretical Biology*, Vol. 462, pp. 499–513.

Alimohammadi, M., Sherwood, J. M., Karimpour, M., Agu, O., Balabani, S., Díaz-Zuccarini, V., 2015. "Aortic dissection simulation models for clinical support: fluid-structure interaction vs. rigid wall models". *BioMedical Engineering OnLine*, Vol. 14, Article number 34, https://doi.org/10.1186/s12938-015-0032-6. Accessed 11 may 2021.

Gebreegziabher, T., Sparrow, E. M., Abraham, J. P., Ayorinde, E. and T. Singh. "High-Frequency Pulsatile Pipe Flows Encompassing All Flow Regimes". *Numerical Heat Transfer Applications*, Vol. 60, pp. 1–16.

Gostuski, V., Pastore, I., Palacios, G. R., Diez, G. V., Moscoso-Vasquez, H. M., Risk, M., 2016. "Time Domain Estimation of Arterial Parameters using the Windkessel Model and the Monte Carlo Method". *Journal of Physics: Conference Series*, Vol. 705, https://iopscience.iop.org/article/10.1088/1742-6596/705/1/012028/meta. Accessed 11 may 2021.

Koegler, A. F., Haselmann, D., Alt, N. S. A., Schluecker, E., 2016. "Experimental Characterization of a Flow-through Pulsation Damper Regarding Pressure Pulsations and Vibrations". *Chemical Engineering Technology*, Vol. 40, No. 1, pp. 162–169.

Ku, D. N., 1997. "Blood Flow in Arteries". *Annual Review of Fluid Mechanics*, Vol. 29, pp. 399–434.

Jahangiri, M., Saghafian, M., Sadeghi, M. R., 2017. "Numerical simulation of non-Newtonian models effect on hemodynamic factors of pulsatile blood flow in elastic stenosed artery". *Journal of Mechanical Science and Technology*, Vol. 31, p. 1003–1013.

Liang, Q., Xiaowei, L., Su, Y., Wu, X., 2020. "Frequency domain analysis of two-phase flow instabilities in a helical tube once through steam generator for HTGR". *Applied Thermal Engineering*, Vol. 168, https://www.sciencedirect.com/science/article/abs/pii/S1359431119352093. Accessed 11 may 2021.

Lorenzini, G., Conti, A., 2013. "Numerical transient state analysis of partly obstructed haemodynamics using FSI approach". *Central European Journal of Engineering*, Vol. 3, pp. 285–305.

Mei, C. C., Zhang, J., Jing, H. X., 2018. "Fluid mechanics of Windkessel effect". *Medical & Biological Engineering & Computing*, Vol. 56, No. 8, pp. 1357–1366.

Nowak, M., Melka, B., Rojczyk, M., Gracka, M., Nowak, A. J., Golda, A., Adamczyk, W. P., Issac, B., Białecki, R. A., Ostrowski, Z., 2019. "The protocol for using elastic wall model in modeling blood flow within human artery". *European Journal of Mechanics / B Fluids*, No. 77, pp. 273–280.

Rao, S., 2009. *Mechanical Vibrations (in Portuguese)*. 4 ed. Pearson Prentice Hall, São Paulo.

Ribas, F. A., Deschamps, C. J., 2004. "Friction Factor Under Transient Flow Condition". In *International Compressor Engineering Conference*, Paper 1665, https://docs.lib.purdue.edu/icec/1665. Accessed 18 may 2021.

Shi, Y., Yang, S., Pan, X., Liu, Y., 2019. "Effects of a Bladder Accumulator on Pressure Pulsation of Urea Dosing System". *IEEE Access*, Vol. 7, pp. 157200-157211.

Thomas, B., Sumam, K. S., 2016. "Blood Flow in Human Arterial System - A Review". *Procedia Technology*, No. 24, pp. 339–346.

Xiaohui, L., Shuping, C., Weijie, S., Xiaofeng, H., 2015. "Analysis and design of a water pump with accumulators absorbing pressure pulsation in high-velocity water-jet propulsion system". *Journal of Marine Science and Technology*, No. 20, pp. 551–558.

Westerhof, N, Lankhaar, J, Westerhof, B. E., 2008. "The arterial Windkessel". *Medical & Biological Engineering & Computing*, Vol. 47, pp. 131–141.

Wachel, J. C., Price, S. M., 1988. "Understanding how pulsation accumulators work". *American Society of Mechanical Engineers, Petroleum Division*, No. 14, pp. 23–31.

Wu, Z., Xiang, Y., Li, M., Iqbal, M. Y., Xu, G., 2019. "Investigation of Accumulator Main Parameters of Hydraulic Excitation System". *Journal of Coastal Research*, Vol. 93, pp. 613–622.

Xu, D., Sun, Y., Liu, Y., Wei, L. 2019. "Analysis of Noise Reduction of Valve-Controlled Hydraulic System for Accumulator Filling". In *IEEE 8th International Conference on Fluid Power and Mechatronics (FPM)*, https://ieeexplore.ieee.org/document/9035775. Accessed 20 march 2021.

Xu, M., Zhang, J., Sun, S., Chen, G., 2018. "Analysis of accumulator effect on the suppression of fluid pulsation". In *2nd IEEE Advanced Information Management, Communicates, Electronic and Automation Control Conference (IMCEC 2018)*, https://ieeexplore.ieee.org/document/8469671. Accessed 19 march 2021.

Zuti, Z., Shuping, C., Huawei, W., Xiaohui, L., Jia, D., Yuquan, Z., 2019. "The approach on reducing the pressure pulsation and vibration of seawater piston pump through integrating a group of accumulators". *Ocean Engineering*, Vol. 173, pp. 319–330.

6. RESPONSIBILITY NOTICE

The authors are the only responsible for the printed material included in this paper.